Characterization and Molecular Profiling of Canine Cancer Cell Lines

Erin Citarella, Sunetra Das, Rupa Idate, & Dawn Duval

Colorado State University, Flint Animal Cancer Center

Abstract

The advent of personalized medicine promises to revolutionize the treatment of cancer but first requires the extensive characterization of a wide range of tumors in order to build an effective framework. Canine cancer cell lines share many similarities to human cancer cell lines and are therefore a valuable resource for expanding the foundation of knowledge that personalized medicine builds off. Utilizing PCR and Sanger sequencing, the presence of a frameshift mutation in exon 20 of the STAT2 gene was confirmed to be conserved across three canine thyroid carcinoma cell lines while mutations in MUC4 and RB1 were not confirmed. Growth inhibition assays of numerous cell lines with Trametinib confirmed the utility of the MPAS in predicting MAPK-inhibitor sensitivity and identification of outlier cell lines. Growth inhibition assays with TK216 lend support for the hypothesis that TK216 works through a more generalized cytotoxic mechanism than first believed, and the reliability of Alamar Blue vs. Incucyte protocols for growth inhibition assays was assessed with Incucyte proving more reliable. Overall, these findings expand the current understanding of the molecular nature of cancer and provide further data for personalized medicine to incorporate to improve future cancer outcomes in both dogs and humans.

Introduction

Human cancer cell lines have been at the forefront of cancer research since their first use in 1951 and have played a critical role in the investigation of the molecular nature of cancer and the development of novel therapeutics (Lyapun, et al. 2020; Mirabelli, et al. 2019). Besides using human cancer cell lines, canine cancer cell lines offer a valuable opportunity for comparative oncology. Canine and human cancers share many genetic and histological similarities, allowing data from research conducted with canine cancer cells to be applied to human disease (Oh & Cho, 2023). Therefore, the characterization of canine cancer cell lines can be used to develop a platform for personalized medicine in both dogs and humans.

While cancer is often viewed as a single monolithic disease, it is really a collection of highly diverse maladies each possessing their own unique genetic, immune, and metabolic landscape. This heterogeneity of disease requires equally diverse therapeutic approaches, which is what personalized medicine strives to achieve. Personalized medicine considers the unique status of each tumor and allows for treatments to be tailored to each patient (Hoeben, et al. 2021). However, the development of this approach requires extensive data about the differences between individual tumors and their therapeutic significance. By identifying the mutations present in different canine cancer cell lines and investigating how these mutations contribute to therapeutic responses, a framework for genetic-based personalized medicine can be developed.

The first part of this project was to confirm the presence of numerous mutations identified by whole exome sequencing (WES) of canine thyroid carcinoma cell lines. This technique involves sequencing of the protein-coding regions of the genome and then comparing this sequencing data to a reference canine genome to identify discrepancies. Previous WES data from the Duval lab identified potential mutations in numerous cell lines. This included seven potential mutations in the Signal transducer and activator of transcription 2 (STAT2) gene, eight cell lines with potential mutations in the Mucin 4, Cell Surface Associated (MUC4) gene, and three cell lines with potential mutations in the Retinoblastoma 1 (RB1) gene. However, WES is subject to error, so subsequent polymerase chain reaction (PCR) and Sanger sequencing must be utilized to confirm the presence of these mutations. Of the potential mutations identified, seven MUC4 mutant cell lines, six STAT2 mutant cell lines, and seven RB1 mutant cell lines were investigated (Figure 1).

STAT2, Exon20, CanFam3					
Tumor ID	*Chromosome*	*Consequence*	*CDNA position*	*Protein position*	*Codons*
TC1593	10	Frameshift	1905-1906	635-636	-/A
TC1593	10	In-frame insertion	1905-1906	635	ctt/ctACAt
TC627	10	Frameshift	1905-1906	635-636	-/A
TC627	10	In-frame insertion	1905-1906	635	ctt/ctACAt
TC2288	10	Frameshift	1905-1906	635-636	-/A
TC2288	10	In-frame insertion	1905-1906	635	ctt/ctACAt
MUC4, Exon1, CanFam4					
Tumor ID	*Chromosome*	*Consequence*	*CDNA position*	*Protein position*	*Codons*
TC2011	33	Missense	1101	352	Gag/Cag
TC2089	33	Missense	1264-1265	406	cTG/cCA
TC1088	33	Missense	300	85	Ggt/Agt
TC2288	33	Missense	1977-1978	644	AGa/TCa
RB1, CanFam3.1					
Tumor ID	*Chromosome*	*Consequence*	*CDNA position*	*Protein*	*Nucleotides*
TC1164	22	Missense	3158674	S222P	A ⇒ G
TC1213	22	Missense	3163280	G195W	C ⇒ A

Figure 1 – Mutations identified by whole exome sequencing (WES) that were selected to be tested using PCR and Sanger sequencing.

STAT2 acts as a transcription factor in response to interferon signaling, which is vital to the cellular antiviral response (NCBI, 2024). When Type I Interferons bind to interferon receptors, Janus kinase 1 (JAK1) and Tyrosine kinase 2 (TYK2) get phosphorylated and activated (Blaszczyk, et al. 2016) . JAK1 and TYK2 can then phosphorylate and activate STAT2. Canonically, when STAT2 gets phosphorylated, it forms a complex with STAT1 and interferon regulatory factor 9 (IRF9) called IFN-stimulated gene factor 3 (ISGF3). The ISGF3 complex then acts as a

transcription factor for over 300 interferon-stimulated genes (ISGs). However, there are also noncanonical pathways where STAT2 forms complexes other than the traditional ISGF3 (Blaszczyk, et al. 2016). STAT2 has been found to be upregulated in various cancers and is associated with poor prognosis in colorectal cancer and melanoma (Chiriac, et al. 2023; Lee, et al. 2020). While the mechanism behind this is not well understood, it is proposed to be due to the tumorigenic effects of inflammatory cytokine production.

MUC4 protein is a membrane protein primarily produced by epithelial cells and involved in the production of mucus (NCBI, 2024). The MUC4 gene is notable for having a 48-nucleotide tandem repeat that can vary greatly in copy number, spanning from 7kb to 19kb in different individuals (Nollet, et al. 1998). MUC4 has been demonstrated to be upregulated in various cancers and associated with poor prognosis in lung adenocarcinoma, pancreatic cancer, and cholangiocarcinoma (cancer of the bile duct) (Carraway, et al. 2010). This is proposed to be due to several mechanisms, including the MUC4 protein blocking the immune system from binding to tumor cells, facilitating metastasis by disrupting cell-cell interactions, and acting as a ligand for Erb-B2 Receptor Tyrosine Kinase 2 (ErbB2). ErbB2 is an epithelial growth factor receptor (EGFR) whose signaling contributes to cell proliferation and differentiation through the mitogen-activated protein kinase (MAPK) and phosphatidylinositol 3-kinase (PI3K) pathways (NCBI, 2024).

RB1 was the first tumor suppressor gene to ever be identified and plays a key role in controlling entry into the cell cycle (NCBI, 2024). RB1 binds to the transcription factor E2F, preventing E2F from activating the expression of genes required to push the cell into S phase (Chinnam & Goodrich, 2011). When RB1 is phosphorylated by cyclin-dependent kinases (CDKs), it releases E2F, and the cell progresses through the cell cycle. Alterations in RB1 expression have been observed in many cancer types and contributes not only to uncontrolled cell proliferation but also tumor metabolism and the tumor immune microenvironment by less well described mechanisms (Knudsen et al. 2020).

The second part of this project was to assess the sensitivity of numerous canine cancer cell lines to the drug Trametinib. Trametinib is an inhibitor of mitogen-activated protein kinase kinase 1 and 2 (MEK1/2), members of the MAPK pathway (Figure 2) (Hoffner & Benchich, 2018). The MAPK pathway is a key signaling pathway involved in cell proliferation and differentiation (Guo, et al. 2020). Mutations in proteins involved in the MAPK pathway are one of the most common mutations across all cancer types and contributes to cancer's characteristic uncontrolled cell proliferation. By inhibiting MEK1 and MEK2, Trametinib decreases MAPK signaling and has been shown to decrease cell proliferation and induce apoptosis in cancer cells (Hoffner & Benchich, 2018).

To better predict the sensitivity of individual cancers to MAPK pathway inhibitors, the MAPK Pathway Activity Score (MPAS) was developed (Wagle, et al. 2018). The MPAS is calculated using the transcript expression levels of ten genes involved in the MAPK pathway (Figure 2) and has been correlated with response to MAPK pathway inhibitors both *in vitro* and *in vivo*.

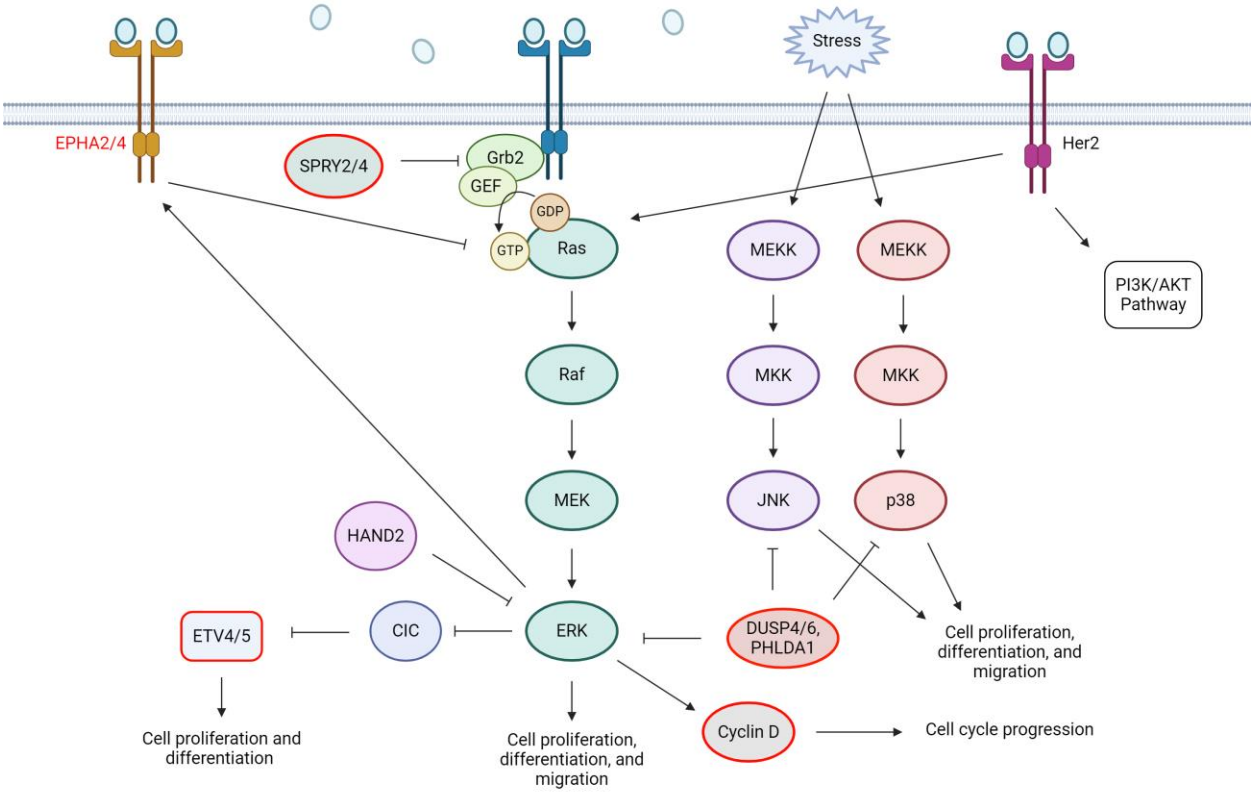

Figure 2 – Diagram of MAPK signaling pathway. Genes used to calculate the MPAS are marked with red borders. Created with BioRender.com

MPAS values were previously calculated for several canine cancer cell lines in the Duval lab but had yet to be validated by drug sensitivity assays. By testing the sensitivity of these cell lines to Trametinib, the reliability of the MPAS score as a predictive biomarker can be assessed as well as allowing for the identification of cell line outliers that may warrant further study. Cell lines CPU98 and CSC165 have high calculated MPAS of 2.18181497 and 2.692637314 respectively. Cell lines COS73 and COS79 have low MPAS of -1.174561433 and -0.8811008779 respectively. CPU185 had no calculated MPAS but is known to have a HER2 mutation like CPU98 and was included out of interest. Kinsey was a positive control as it has a high MPAS of 4.149239267 and has previously been shown to be highly sensitive to Trametinib.

The third part of the project was investigating the Capicua Transcriptional Repressor (CIC) gene in the B-cell lymphoma cell line 1771. 1771 has previously been observed to have a high calculated MPAS, but a low sensitivity to Trametinib. Looking closer at the individual genes covered by the MPAS, 1771 has very high expression of the oncogenic transcription factors ETV4 and ETV5 (Figure 3). The whole exome sequencing data also shows a mutation in the CIC gene, which is a known repressor of ETV4 and ETV5, in 1771 (Bunda, et al. 2019). The CIC gene in 1771 is fused with the class II major histocompatibility complex transactivator (CIITA). It is hypothesized that the CIC mutation in the 1771 cell line is leading to increased expression of ETV4

and ETV5, which is in turn leading to an increased calculated MPAS even though the MAPK pathway is activated downstream of Trametinib's targets rendering the cell line insensitive to the drug. To investigate this further, drug sensitivity assays were performed using the drug TK-216, an inhibitor of ETS transcription factors including ETV4 and ETV5 (Spriano, et al. 2019). The cell line CLL1390 was used as a negative control, since this is a lymphoma cell line with a low MPAS and no CIC mutation. PCR and Sanger sequencing will also be used to confirm the presence of the CIC gene fusion in the 1771 cell line. This project is currently in progress.

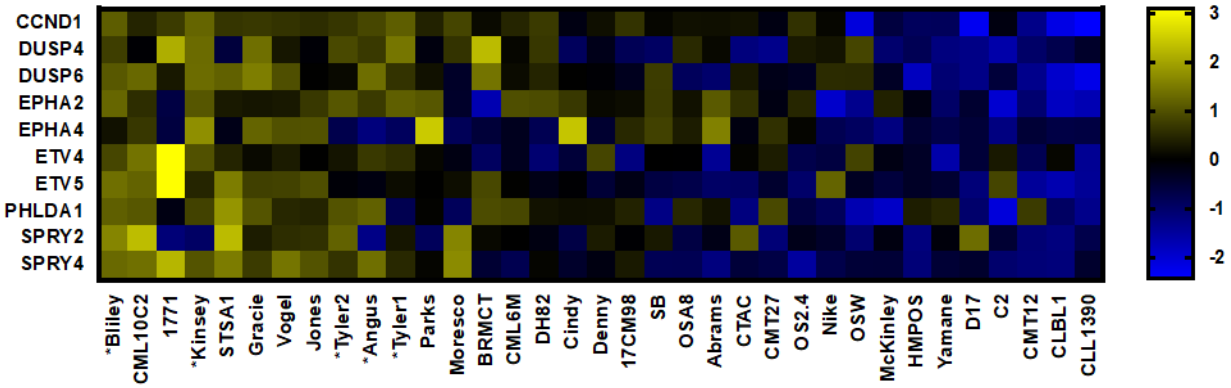

Figure 3 – Heatmap showing gene expression levels of 10 genes used to calculate MPAS in previously investigated cell lines. Note the high expression of ETV4 and ETV5 in the 1771 cell line.

Methods and Materials

Cell Lines and Culture

Cell lines CPU98, CSC165, COS73, COS79, and CPU185 were established in the Flint Animal Cancer Center (FACC) at Colorado State University. Kinsey cell line was established by Tufts University, 1771 cell line was established by the University of Pennsylvania, and CLL1390 cell line was established by UC Davis. Cells were cultured in Dulbecco's Modified Eagle Medium (DMEM) +4 mM L-Glutamine, +2500 mg/L Glucose and -Sodium Pyruvate with 10% fetal bovine serum (FBS) and 5% antibiotics (gibco Antibiotic-Antimycotic 100X). Media was supplemented with Corning MEM Nonessential Amino Acids 100 X Solution, Corning MEM Vitamins 100 X Solution, and Corning Sodium Pyruvate 100 mM Solution.

Whole Exome Sequencing

Whole exome sequencing (WES) was previously conducted (not by the student) by capturing exonic regions from fragmented genomic DNA using the 43.45 Mb custom Agilent SureSelect XT All Exon V2 (part number: 931198) capture kit. Read quality was assessed by FastQC and Trimmomatic was used to select high-quality reads (phred score >20) and eliminate adapter sequences. The high-quality reads were mapped against the canine genome (v3.1) using BWA tool. Preprocessing of alignment files for variant calling was done in accordance with GATK best practices (Van der Auwera, et al. 2013). Freebayes was used to call variants with a min-alternate-

count of 2 and min-alternate-fraction of 0.05. Identified variants were filtered for depth of >10 and QUAL >20 and annotated with SnpEff.

PCR and Sanger Sequencing

Primers for PCR were designed using Primer3Plus and Geneious using whichever canine reference genome was used for WES for each set of mutations. Primers were run through NCBI BLAST to determine possible off-target binding sites. PCR ran on 1.2% agarose gel at a melting temperature determined by the specific primer sets used each time. Qiagen DNA extraction kit used to extract DNA from fragment band on gel (correct band identified by size comparison with DNA ladder). Nanodrop was used to measure DNA concentration before samples were prepared and sent to Azenta Life Sciences for Sanger sequencing. Sequencing data was analyzed using Geneious software.

MAPK Pathway Activity Score

MPAS is calculated using transcript levels of 10 genes involved in the MAPK pathway as described in the Wagle, et al. 2018 paper. The 10 genes are PHLDA1, SPRY2, SPRY4, DUSP4, DUSP6, CCND1, EPHA2, EPHA4, ETV4, and ETV5. MPAS computed as MAPK = $\frac{\Sigma_i^z}{\sqrt{n}}$ where z_i is the z-score of each gene's expression level and n is the number of genes comprising the set (i.e., n = 10). This means that the MPAS is a relative value based on the samples included.

Growth Inhibition Assays

Trametinib and TK216 drugs were obtained from Selleck Chemicals. Drugs were dissolved in dimethyl sulfoxide (DMSO) and DMSO was used was a control. Cell lines CPU98, CSC165, COS73, COS79, CPU185, and Kinsey were treated with serial dilutions of Trametinib ranging from 10 µM to 7.6295 x 10^{-5} µM. Cells were treated one day after plating them at 1000 cells per well. Cell confluence was read at time zero (day of treatment) and on day 5 using the Incucyte system. Suspension cell lines 1771 and CLL1390 were treated with serial dilutions of TK216 ranging from 2 µM to 3.38702 x 10^{-5} µM. Cells were treated the same day as being plated at 2000 cells per well. Cell viability was assessed at time zero and day 3 using Alamar blue. Cells were incubated with Alamar blue for 3-4 hours and absorbance was measured using a standard plate reader.

Growth Inhibition Data Analysis

Data from growth inhibition assays was analyzed using Microsoft Excel software. The blank readings were subtracted and averages for each drug concentration calculated. Fold change was calculated by dividing the final averages by the time zero averages. The fraction of control was calculated by dividing each fold change value by the fold change of the DMSO control wells. This was then multiplied by 100 to give the percent fraction of control.

Data was then further analyzed using the GraphPad Prism software. The percent fraction of control values were used and the drug concentrations were converted to logarithms. A non-linear regression curve was obtained and is displayed in the graph. IC50s were also calculated using the GraphPad Prism software.

Results

PCR and Sanger Sequencing confirmed the presence of the STAT2 mutation in Exon 20 in the cell lines TC1593, TC2288, and TC627 (Figure 4). The mutations in RB1 were found not to be present in the tested cell lines TC1164 and TC1213 (Figure 5). Amplification and sequencing of the MUC4 gene proved difficult, and it was not confirmed whether or not any MUC4 mutations were present.

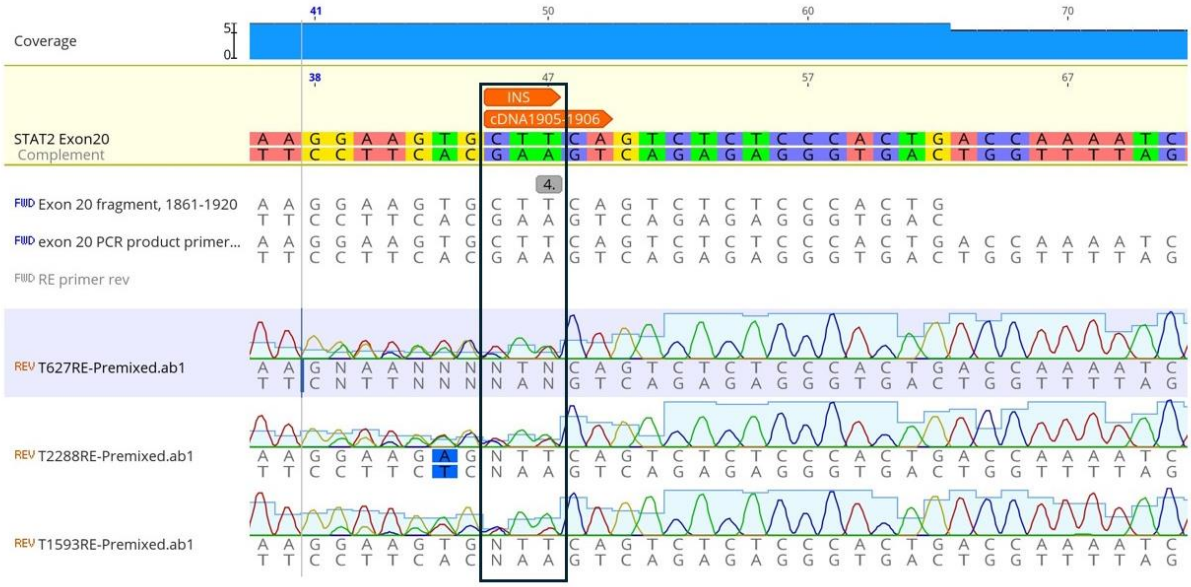

Figure 4 – Sanger sequencing results for STAT2 Exon 20 mutation for cell lines TC627, TC2288, and TC1593, confirming the presence of a shared frameshift mutation. Geneious software used.

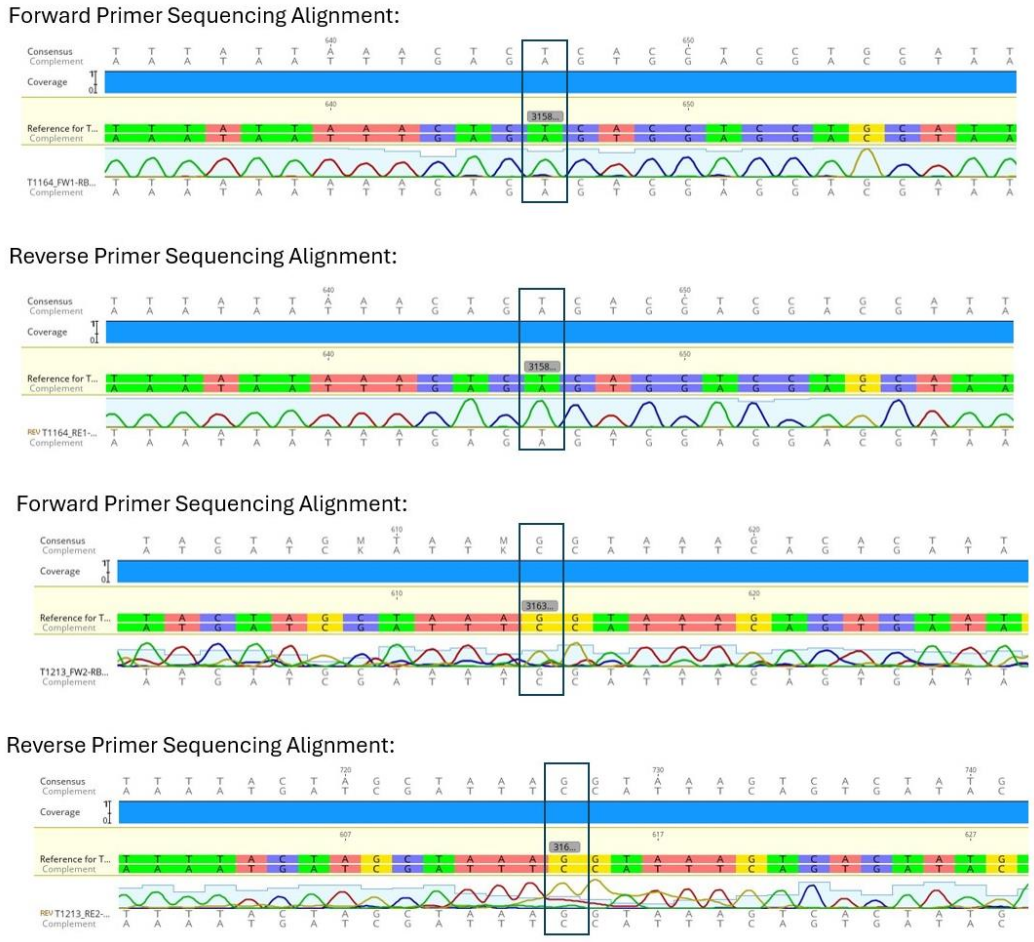

Figure 5 - Sanger sequencing results for RB1 mutation for cell lines TC1164 (top) and TC1213 (bottom), revealing the absence of a mutation in the RB1 gene. Geneious software used.

The Trametinib growth inhibition assay of the cell lines CPU98, CPU185, CSC165, COS73, COS79, and Kinsey largely showed the expected results (Figure 6). The two cell lines with low MPAS, COS73 and COS79, were the least sensitive to Trametinib. The CSC165 cell line had a high MPAS and was similarly sensitive to Trametinib as the positive control Kinsey cell line. CPU98 was not as sensitive to Trametinib as expected based on its high MPAS, but this could be explained by the presence of a HER2 mutation in this cell line. HER2 is a receptor tyrosine kinase implicated in carcinogenesis as it can activate both MAPK and the PI3K pathways (Kirouac, et al. 2016). While Trametinib targets the MAPK pathway, the HER2 mutation in the CPU98 cell line could allow it to continue utilizing the PI3K pathway and exhibit some resistance to the drug despite its high MPAS. The cell line CPU185 did not have a calculated MPAS, though it is known to also possess a HER2 mutation. Both CPU98 and CPU185 responded similarly to Trametinib, possibly through the same PI3K-activating HER2 mechanism. The IC50 values for each cell line were 0.003 uM for CPU98, 0.027 uM for CPU185, 0.002 uM for CSC165, 9.67 uM for COS79, and 0.002 uM for Kinsey. The IC50 for COS73 couldn't be calculated since it never reached 50% growth inhibition.

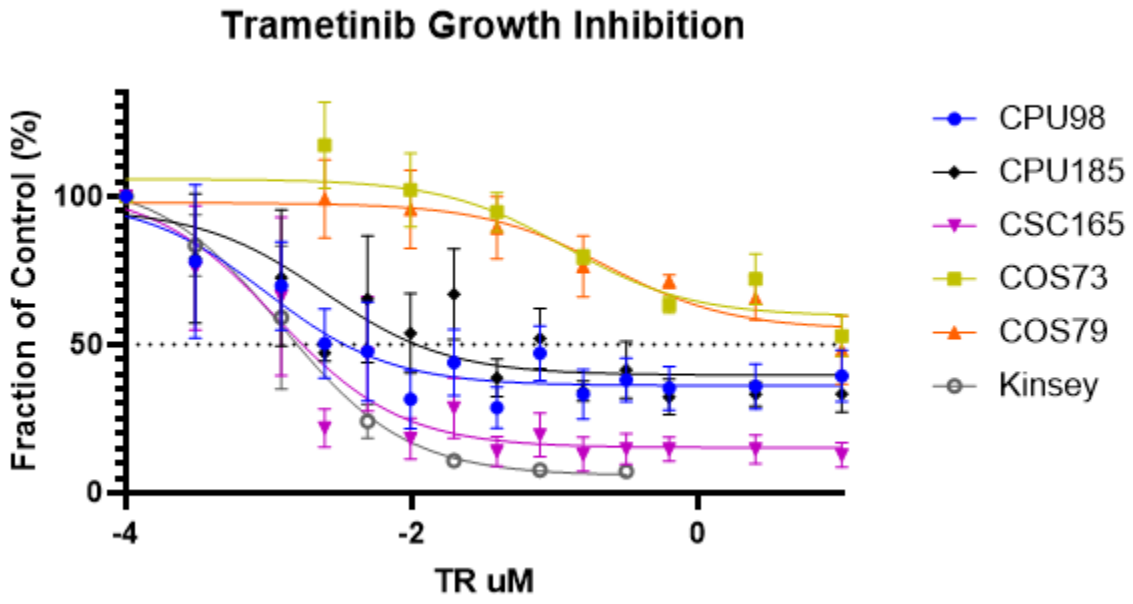

Figure 6 – Nonlinear regression curve of Trametinib growth inhibition data from Incucyte cell confluence readings.

Figure 7 shows the results of the TK216 growth inhibition assay of the cell lines 1771 and CLL1390. While the Incucyte system was used for data collection in the Trametinib assays, 1771 and CLL1390 are suspension cell lines and therefore are not as conducive to cell confluence measurements. Instead, an Alamar blue assay was utilized. Unfortunately, this technique proved to be problematic due to issues with the plate reader used, indicated by the large error bars in the figure. However, despite the questionable reliability of this assay, the 1771 and CLL1390 cell lines appear to respond similarly to the TK216 drug. This was initially surprising as the 1771 cell line's CIC mutation and high ETV4 and ETV5 expression should make it more sensitive to the ETS inhibitor TK216 than the low MPAS, non-CIC mutant CLL1390 control cell line. However, upon further investigation, it appears that the TK216 drug is not as specific as initially thought. Besides inhibiting specific transcription factors, TK216 may also function as a microtubule-destabilizing agent (Povedano, et al. 2022). This mechanism of action would be non-specific and could explain the sensitivity observed in the CLL1390 cell line.

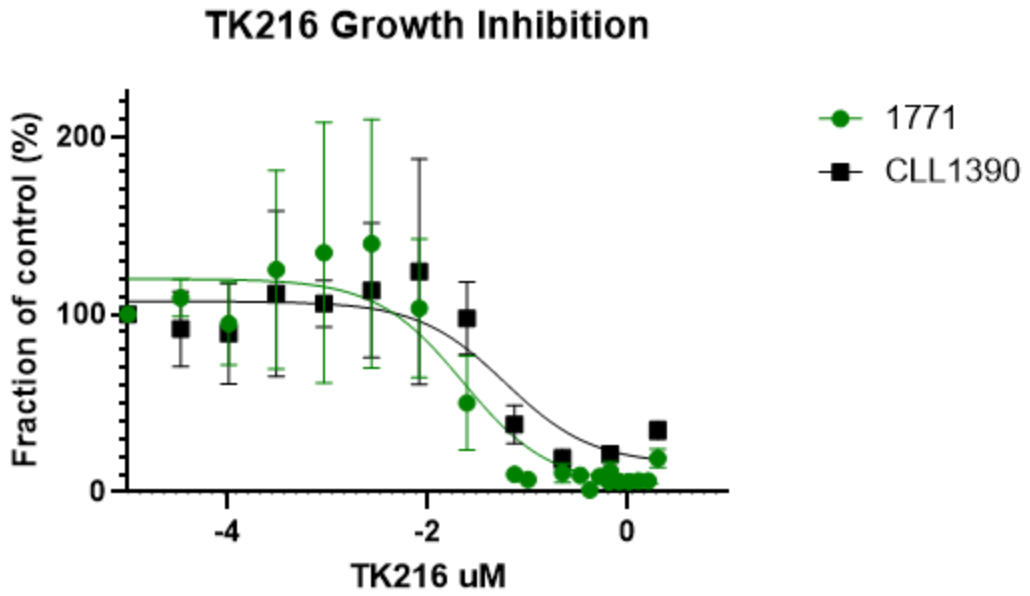

Figure 7 - Nonlinear regression curve of TK216 growth inhibition data.

Discussion

The presence of a frameshift mutation in Exon 20 of the STAT2 gene was confirmed in three separate canine thyroid carcinoma cell lines. While the relevance of this mutation to oncogenesis and disease progression is unclear, it certainly warrants future study. Further characterization of this mutation and its impacts may provide avenues for personalized medicine.

The absence of RB1 mutations in the two cell lines tested was also an interesting finding. As a tumor suppressor, RB1 is highly relevant to cancer. A mutation in this gene would likely be a major contributor to oncogenesis. However, the wild type RB1 genes found in these cell lines suggests another driving mechanism that has yet to be elucidated.

The most challenging gene to investigate was the MUC4 gene. This gene has a 48-nucleotide tandem repeat that can vary greatly in copy number and presents a significant obstacle to PCR amplification. Primers targeted to the potential mutation's specific location will also bind elsewhere in the gene, leading to multiple amplified fragments (Figure 8). Despite numerous rounds of primer design and testing of mutations at different locations, clean amplification remained unsuccessful.

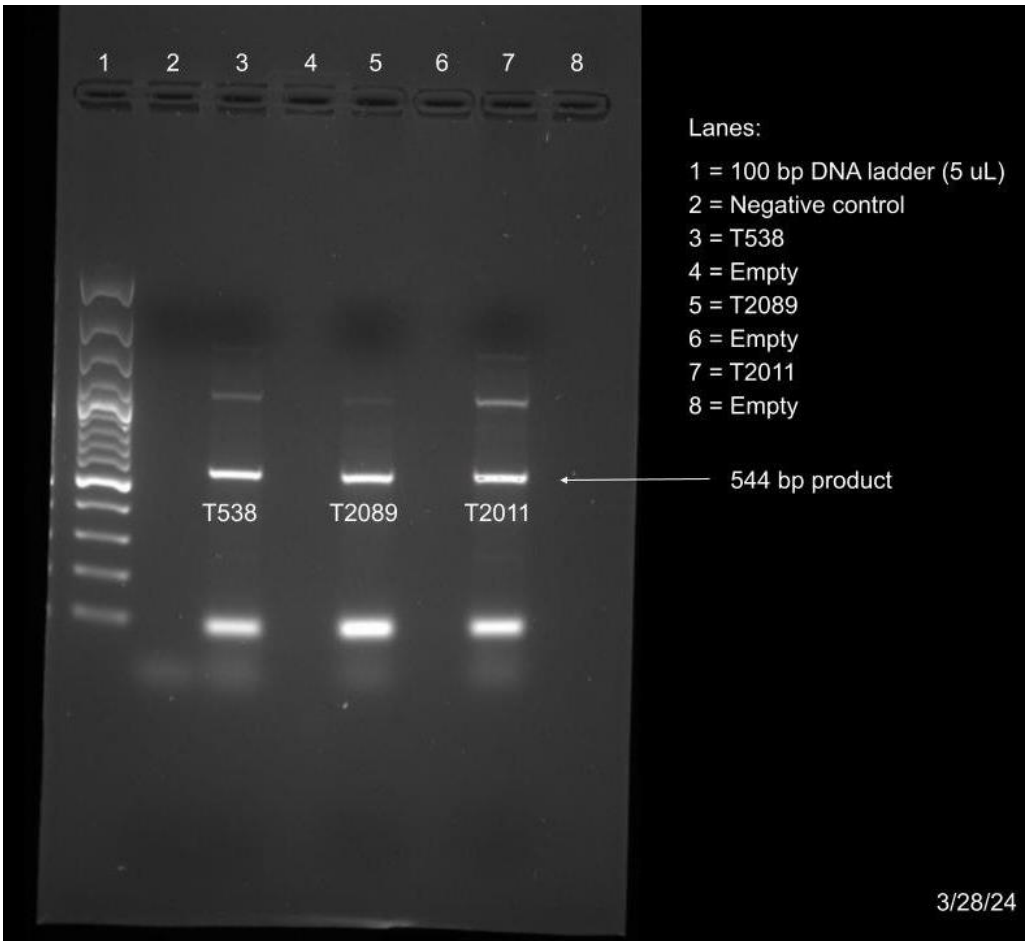

Figure 8 – Gel electrophoresis of PCR-amplified MUC4 gene fragments in tumor samples TC538, TC2089, and TC2011. While the 544 bp band was the product of interest, numerous other bands are present from off-target binding of primers.

The results of the Trametinib growth inhibition assays support the reliability and utility of the MAPK Pathway Activity Score (MPAS). The cell lines with low MPAS were resistant to the MEK1/2 inhibitor Trametinib, while the cell lines with high MPAS were sensitive to the drug. The CPU98 cell line did not behave exactly as expected, but this can be explained by the presence of a HER2 mutation in this cell line. HER2's activation of the PI3K pathway may allow this cell line to grow better than expected even when the MAPK pathway is inhibited. As the cell line CPU185 also possesses a HER2 mutation and displayed very similar Trametinib sensitivity to CPU98, these cell lines likely utilize the same mechanism for partial resistance. Based on these experimental results, the MPAS is not only a valuable predictor of MAPK-pathway inhibitor response in cancer cells but also a useful tool for identifying cell lines with alternative driving mechanisms.

While the TK216 growth inhibition assays of 1771 and CLl1390 did not show the expected results, they did provide evidence supporting the hypothesis that the ETS-inhibitor TK216 has non-specific cytotoxic effects. The 1771 cell line has high expression of ETV4 and ETV5 as the result of a CIC mutation and this is hypothesized to be the driving mechanism of this cell line. The CLL1390 cell line was included as a negative control, as it has no known CIC mutation, a low

MPAS, and low expression of ETV4 and ETV5. However, despite these differences, both the 1771 and CLL1390 cell lines responded similarly to the TK216 drug. This suggests a more generalized mechanism for cytotoxicity besides just inhibiting specific transcription factors. Other studies have come out suggesting the same thing, specifically that TK216 may act as a microtubule-destabilizing agent (Povedano, et al. 2022). The results of this experiment lend further support to this theory.

The largest obstacle faced by this project was the method used for measuring growth inhibition of the cell lines in both the Trametinib and TK216 assays. Initially, the Alamar Blue assay was used for the Trametinib assays since this was the default method utilized by the Duval lab and it had previously proved reliable. However, the results from the initial experiments were inconsistent and confounding. The cells treated with the highest dose of drug were growing better than the control, which was very unexpected. After repeating this assay five times and obtaining the same results, the Kinsey cell lines were introduced as a positive control. These cells had previously displayed high sensitivity to Trametinib and had not yielded any unexpected results, so by including them in the assay it could be determined whether the data was accurate or not. After repeating the assay several more times with the Kinsey cell included, the data did not improve, and it was determined that the problem lay with the assay protocol itself (Figure 9). It is important to note that while the data was highly variable and continued to exhibit strange patterns, it did show a bit of separation between the sensitive and resistant cell lines. The data is not reliable enough to draw strong conclusions from, but it does show the low MPAS cell lines COS73 and COS79 as being less sensitive than the high MPAS CPU98, CSC165, and Kinsey cell lines. The positive control Kinsey cell lines did demonstrate strong sensitivity as would be expected, even if the data continued to suggest that the cells grew better as the drug dose increased.

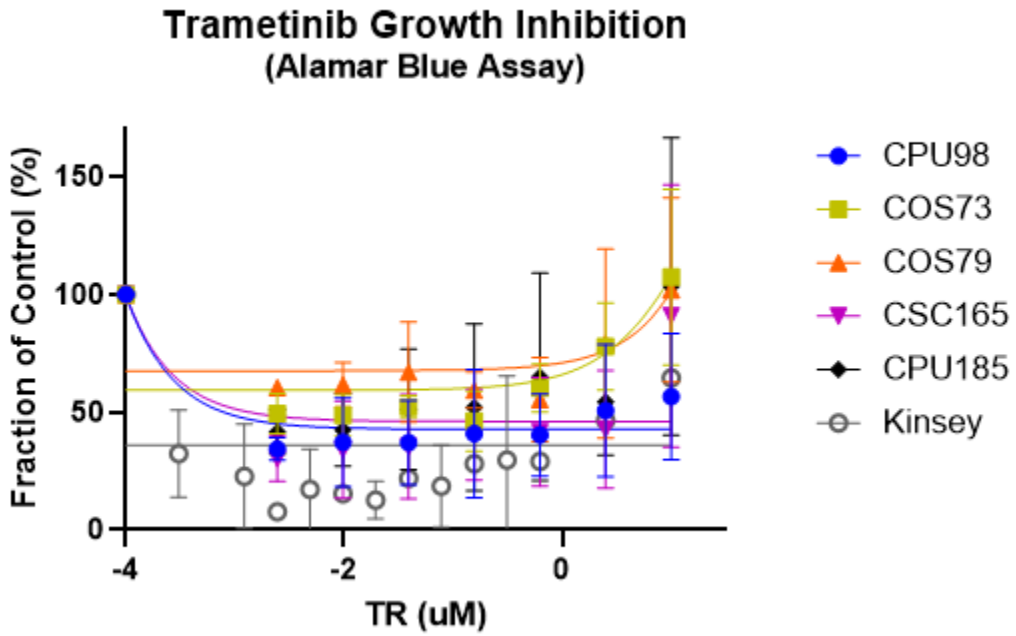

Figure 9 – Plate reading data from Trametinib growth inhibition assays. Cells plated at 2000 cells per well and incubated with drug for 3 days before reading using Alamar Blue protocol. Several outlier data points excluded. Note the untraditional curve of the graph, with cells growing better at higher drug concentrations.

Numerous steps were taken to troubleshoot the protocol besides including the Kinsey cell lines. Different pipettes and reservoirs were used in case they were contaminated. The Trametinib drug was diluted 10X before diluting it again for the treatment concentrations in case the problem was pipetting error with small volumes. The max drug treatment molarity was also quadrupled for one repeat to see if the pattern continued even at such high doses, which it did. The entire protocol and technique were observed by other researchers to ensure proper practice, and no problems were identified. Different numbers of cells and days of incubation with the drug treatment were also adjusted, as well as the time between treatment with Alamar Blue and reading, to no avail. New Alamar Blue solution was prepared in case the problem lay with the reagent, but despite preparing new solutions multiple times the issues were not resolved. Different protocols on the plate reader were also utilized, including extending the read time and changing the absorbance wavelengths to read. The plates were also put on a shaker before reading to ensure the wells were well mixed. A test plate was prepared with 96 identical wells of 2000 cells per well of CPU98 in 200 µL of media and this was read by the plate reader. When read in the proper orientation, the plate displayed inconsistent results with a standard deviation of 1850.51. When the plate was turned in the plate reader, the standard deviation was much lower at 538.09. Even though the exact same wells were read by the exact same protocol mere minutes apart, the results were quite different. This further supported the theory that the problem lay with the plate reader. The plates then started being read by the Incucyte system and the plate reader in conjunction. The data yielded by the Incucyte system exhibited the expected growth curve pattern and much smaller error bars, even while the exact same plates read using the Alamar Blue protocol continued exhibiting inconsistent results. Eventually it was decided to use the Incucyte system exclusively, from which the final Trametinib growth inhibition graphs were obtained.

While the Incucyte system worked well for the adherent cell lines, it was not usable for the TK216 assays using the suspension cell lines 1771 and CLL1390. The Incucyte system reads the cell confluence on the bottom of each well, but suspension cell lines have cells dispersed throughout the media and do not adhere to the bottom for reading. Even if the plates were spun so that the cells went to the bottom, there would be no way to know which cells were alive and which were dead. Alternative methods and reagents were investigated, but ultimately it was decided not to pursue them. After learning that the TK216 drug was not as highly specific as once thought, it became a lower priority experiment that was not worth spending extra money on. While the plate reading data from the Alamar Blue protocol with these assays is not ideal, exhibiting heinously large error bars, it is sufficient for the purposes of this experiment. As the initial plate reading data from the Trametinib assays did display a separation between sensitive and resistant cell lines that was confirmed by the Incucyte data, it can be assumed that the TK216 plate reading data is equally representative. While accurate IC50s cannot be calculated, the response of the 1771 and CLL1390 cell lines appears to be very similar, as would be expected by a generally cytotoxic drug. It is

possible that one cell line or the other is marginally more sensitive, though this cannot be determined from the unreliable plate reading data alone. Either way, the difference between the cell lines is not nearly as profound as would be expected from an ETS-specific drug, supporting the hypothesis of TK216 being generally cytotoxic.

Despite the obstacles, this project yielded valuable findings. A frameshift mutation in Exon20 of the STAT2 gene was found in three separate canine thyroid carcinoma cell lines. The Trametinib growth inhibition assays confirmed not only that the MPAS is a valuable tool for predicting sensitivity to MAPK-inhibitors but also identifying outlier cell lines driven by alternative mechanisms. The TK216 assays provided further support for the hypothesis that TK216 acts through a more general cytotoxic mechanism rather than as a specific ETS inhibitor. The reliability of methods was also assessed, finding that the Incucyte system was more reliable than the Alamar Blue plate reading protocol. Overall, these findings advance the understanding of the molecular mechanisms of cancer and contribute towards building a framework for personalized medicine in both dogs and humans.

References

Blaszczyk K, Nowicka H, Kostyrko K, Antonczyk A, Wesoly J, Bluyssen HAR. The unique role of STAT2 in constitutive and IFN-induced transcription and antiviral responses. *Cytokine Growth Factor Rev*. 29:71-81 (2016). doi: 10.1016/j.cytogfr.2016.02.010.

Bunda, S., Heir, P., Metcalf, J. et al. CIC protein instability contributes to tumorigenesis in glioblastoma. *Nat Commun.* 10, 661 (2019). doi: 10.1038/s41467-018-08087-9

Carraway KL, Theodoropoulos G, Kozloski GA, Carothers Carraway CA. Muc4/MUC4 functions and regulation in cancer. *Future Oncol.* 5(10):1631-40 (2009). doi: 10.2217/fon.09.125.

Chinnam M & Goodrich DW. Chapter 5 - RB1, Development, and Cancer. *Curr Top Dev Biol.* 94:129-169 (2011). doi: 10.1016/B978-0-12-380916-2.00005-X.

Chiriac MT, Hracsko Z, Becker C, Neurath MF. STAT2 Controls Colorectal Tumorigenesis and Resistance to Anti-Cancer Drugs. *Cancers (Basel).* 15(22):5423 (2023). doi: 10.3390/cancers15225423.

Guo YJ, Pan WW, Liu SB, Shen ZF, Xu Y, Hu LL. ERK/MAPK signalling pathway and tumorigenesis (Review). *Exp Ther Med*. 19(3):1997-2007 (2020) doi: 10.3892/etm.2020.8454

Hoeben A, Joosten EAJ, van den Beuken-van Everdingen MHJ. Personalized Medicine: Recent Progress in Cancer Therapy. *Cancers.* 13(2):242 (2021). doi: 10.3390/cancers13020242

Hoffner B, Benchich K. Trametinib: A Targeted Therapy in Metastatic Melanoma. *J Adv Pract Oncol*. 9(7):741-745 (2018). PMID: 31249721 PMCID: PMC6570520

Kirouac DC, Du J, Lahdenranta J, Onsum MD, Nielsen UB, Schoeberl B, McDonagh CF. HER2+ Cancer Cell Dependence on PI3K vs. MAPK Signaling Axes Is Determined by Expression of EGFR, ERBB3 and CDKN1B. *PLoS Comput Biol*. 12(4):e1004827 (2016). doi: 10.1371/journal.pcbi.1004827.

Knudsen, E.S., Nambiar, R., Rosario, S.R. et al. Pan-cancer molecular analysis of the RB tumor suppressor pathway. *Commun Biol.* 3, 158 (2020). doi: 10.1038/s42003-020-0873-9

Lee, CJ., An, HJ., Cho, E.S. et al. Stat2 stability regulation: an intersection between immunity and carcinogenesis. *Exp Mol Med.* 52, 1526–1536 (2020). doi: 10.1038/s12276-020-00506-6

Lyapun, I.N., Andryukov, B.G. & Bynina, M.P. HeLa Cell Culture: Immortal Heritage of Henrietta Lacks. *Mol. Genet. Microbiol. Virol.* 34, 195–200 (2019). doi: 10.3103/S0891416819040050

Mirabelli P, Coppola L, Salvatore M. Cancer Cell Lines Are Useful Model Systems for Medical Research. *Cancers (Basel)*. 11(8):1098 (2019). doi: 10.3390/cancers11081098.

NCBI. ERBB2 erb-b2 receptor tyrosine kinase 2 [Homo sapiens (human)] Gene ID: 2064. *NCBI*. (2024)

NCBI. MUC4 mucin 4, cell surface associated [Homo sapiens (human)] Gene ID: 4585. *NCBI*. (2024)

NCBI. RB1 RB transcriptional corepressor 1 [Homo sapiens (human)] Gene ID: 5925. *NCBI*. (2024)

NCBI. STAT2 signal transducer and activator of transcription 2 [Homo sapiens (human)] Gene ID: 6773. *NCBI*. (2024)

Nollet S, Moniaux N, Maury J, Petitprez D, Degand P, Laine A, Porchet N, Aubert JP. Human mucin gene MUC4: organization of its 5'-region and polymorphism of its central tandem repeat array. *Biochem J.* 1998 Jun 15;332(Pt 3):739–748. doi: 10.1042/bj3320739

Oh, J.H., Cho, JY. Comparative oncology: overcoming human cancer through companion animal studies. *Exp Mol Med* 55, 725–734 (2023). doi: 10.1038/s12276-023-00977-3

Povedano JM, Li V, Lake KE, Bai X, Rallabandi R, Kim J, Xie Y, De Brabander JK, McFadden DG. TK216 targets microtubules in Ewing sarcoma cells. *Cell Chem Biol.* 29(8):1325-1332.e4 (2022). doi: 10.1016/j.chembiol.2022.06.002.

Spriano F, Chung EYL, Gaudio E, Tarantelli C, Cascione L, Napoli S, Jessen K, Carrassa L, Priebe V, Sartori G, Graham G, Selvanathan SP, Cavalli A, Rinaldi A, Kwee I, Testoni M, Genini D, Ye BH, Zucca E, Stathis A, Lannutti B, Toretsky JA, Bertoni F. The ETS Inhibitors YK-4-279 and TK-216 Are Novel Antilymphoma Agents. *Clin Cancer Res*. 25(16):5167-5176 (2019). doi: 10.1158/1078-0432.CCR-18-2718.

Van der Auwera GA, Carneiro MO, Hartl C, Poplin R, Del Angel G, Levy-Moonshine A, et al. From FastQ data to high confidence variant calls: the Genome Analysis Toolkit best practices pipeline. *Curr Protoc Bioinfor-matics* 43:11.0.1–33 (2013) doi: 10.1002/0471250953.bi1110s43

Wagle, MC., Kirouac, D., Klijn, C. et al. A transcriptional MAPK Pathway Activity Score (MPAS) is a clinically relevant biomarker in multiple cancer types. *npj Precision Onc* 2, 7 (2018). doi: 10.1038/s41698-018-0051-4

Zeiser, R., Andrlová, H., Meiss, F. (2018). Trametinib (GSK1120212). In: Martens, U. (eds) Small Molecules in Oncology. *Recent Results in Cancer Research*, vol 211. Springer, Cham. doi: 10.1007/978-3-319-91442-8_7